Discrimination of Atoms on the Surface of a Two-Dimensional Solid Solution with Scanning Tunneling Microscopy

B. A. Parkinson

Contribution No. 5143 from the Central Research and Development Department, E.I. du Pont de Nemours & Company, P.O. Box 80328, Wilmington, Delaware 19880-0328.
Received April 25, 1989

Abstract: Atomic resolution scanning tunneling microscope (STM) images of WS_2, WSe_2, and the solid solution WSeS were obtained in air. The statistical distribution of the peak tunneling currents at each atom location was much larger for the solid solution than for the pure phases. A clearly separated bimodal distribution was not observed for WSeS, and so surface occupancies could not be unambiguously assigned. A model relating the magnitude of the tunneling current of a given atom to its identity and nearest-neighbor environment was then developed. Computer-simulated images using this model were compared with the real images. From the model, sulfur and selenium positions for the imaged surface could then be deduced for >90% of the surface atoms. The occupancy appeared to be random as was expected for a solid solution. Speculative applications for the ability to discriminate surface atoms are discussed.

The ultimate surface analysis technique would be capable of distinguishing individual atoms on a surface. The key step toward this goal was taken with the invention of the scanning tunneling microscope (STM).[1] Usually the STM is used to identify the surface symmetry of homogeneous atomic surfaces; however, several examples of atomic recognition have appeared in the literature. Most of these examples are concerned with the identification of impurity atoms,[2] defects,[3] or adsorbates.[4] In this paper we will attempt to elucidate the surface atomic structure of a near equimolar solid solution of the 2D materials 2H-WS_2 and 2H-WSe_2.

The 2D structure of these transition-metal dichalcogenides provides several key advantages for fundamental surface studies: atomic flatness due to the van der Waals nature of their (0001) surfaces, inertness to reactions with ambient air and water, and renewability via easy cleavage. The naturally occurring material MoS_2 has already been shown to be an excellent substrate for obtaining atomic resolution with the STM in air,[7] as has the structurally related material $NbSe_2$.[8] α-$MoTe_2$ and WTe_2, because of their different metal sublattice symmetries, have been used to demonstrate that tunneling to subsurface metal atoms is possible.[9] Charge density waves (simultaneously with surface atoms) can be observed on TaS_2 and several other metallic 2D materials.[10] So it is apparent that this class of materials has a richness of structural and electronic properties not available in another common 2D substrate for STM imaging, graphite, although in our hands atomic resolution on these materials is not quite as routine as on graphite but still is much easier than on an intrinsically 3D material.

Table I

data set	WSeS no. 1	WSeS no. 2	WSe_2
no. of atoms	209	237	134
min[a]	70	65	70
max[a]	240	185	85
mean[a]	167	116	77
std error	1.70	1.31	0.28
variance	601	408	10.6
std dev	24.5	20.2	3.3
coeff of variance	14.6	17.5	4.2

[a] Arbitrary units proportional to tunneling current in the constant-height mode of the STM.

Experimental Section

Crystals of the material WSeS were grown by sealing stoichiometric amounts of the elements into a quartz ampule with Cl_2 as a transporting agent, heating the contents to 1000 °C for 1 week, and then transporting crystals with hot- and cold-zone temperatures of 1020 and 915 °C, respectively. The stoichiometry of the material was verified by electron microprobe analysis by averaging the results from several areas on four crystals. The average composition was found to be $WSe_{0.96}S_{1.04}$, but the material will be referred to as WSeS.[11]

The scanning tunneling microscope used was a Nanoscope II manufactured by Digital Instruments, Santa Barbara, CA. The crystal samples (3 × 3 mm) were mounted to copper disks with Ag epoxy and cleaved via sticky tape before each STM experiment. Electrochemically etched platinum tips were prepared by placing Pt wire in a 5 M KCN-2 M KOH solution and etching them with 2.5-V ac at an initial current of greater than 45 mA. The current gradually decays to zero when the tip is complete, usually in less than 15 min. A similar method was reported by Lewis et al. for etching Pt-Ir tips, but this material requires much higher voltages and currents.[12] All images of the solid solution surface were obtained in the constant-height mode with a bias voltage between -700 and -900 mV and a tunneling current of 1-3 nA. Attempts to obtain atomic resolution images for the mixed-atom substrates at positive biases were unsuccessful even though atomic resolution could be obtained on the pure substrates with either tip polarity.

The computer program for simulating atom positions and gray scales was written in Z Basic on a Macintosh computer with a Laserwriter for graphic output.

Results and Discussion

Figure 1 shows both filtered and unfiltered constant-height STM current images of freshly cleaved surfaces of the solid solution WSeS and the pure phases WS_2 and WSe_2. Clear atomic resolution is obtained in all cases, and such images are reproducible from scan to scan, sample to sample, cleave to cleave, and tip to

(1) Binning, G.; Rohrer, H.; Gerber, Ch.; Weibel, E. *Phys. Rev. Lett.* **1982**, *49*, 57.
(2) Stroscio, J. A.; Feenstra, R. M.; Fein, A. P. *Phys. Rev. Lett.* **1987**, *58*, 1668. Stroscio, J. A.; Feenstra, R. M.; Newns, D. M.; Fein, A. P. *J. Vac. Sci. Technol. A* **1988**, *6*, 499.
(3) Drake, B.; Sonnenfeld, R.; Schnair, J.; Hansma, P. K.; Slough, C. G.; Coleman, R. V. *Rev. Sci. Instrum.* **1986**, *55*, 441.
(4) Wolkow, R.; Avouris, Ph. *Phys. Rev. Lett.* **1988**, *60*, 1049.
(5) Stupian, G. W.; Leung, M. S. *Appl. Phys. Lett.* **1987**, *51*, 1560.
(6) Weimer, M.; Kramar, J.; Bai, C.; Baldeschweiler, J. D. *Phys. Rev. B: Condens. Matter* **1988**, *37*, 8.
(7) Sarid, D.; Henson, T. D.; Armstrong, N. R.; Bell, L. S. *Appl. Phys. Lett.* **1988**, *52*, 2252.
(8) Dahn, D. C.; Watanabe, M. O.; Blackford, B. L.; Jericho, M. H. *J. Appl. Phys.* **1988**, *63*, 315.
(9) Tang, S. L.; Kasowski, R. V.; Parkinson, B. A. *Phys. Rev. B.*, in press.
(10) Coleman, R. V.; Drake, B.; Hansma, P. K.; Slough, G. *Phys. Rev. Lett.* **1985**, *55*, 394. Slough, C. G.; McNairy, W. W.; Coleman, R. V.; Drake, B.; Hansma, P. K. *Phys. Rev. B.: Condens. Matter* **1986**, *34*, 994. Giambattista, B.; Johnson, A.; Coleman, R. V.; Drake, B.; Hansma, P. K. *Phys. Rev. B: Condens. Matter* **1988**, *37*, 2741. Wu, X. L.; Lieber, C. M. *J. Am. Chem. Soc.* **1988**, *110*, 5200. Wu, X. L.; Zhou, P.; Lieber, C. M. *Nature* **1988**, *335*, 55. Parkinson, B. A. Unpublished results.
(11) Kline, G.; Kam, K.; Ziegler, R.; Parkinson, B. A. *Sol. Energy Mater.* **1982**, *6*, 337.
(12) Penner, R. M.; Heben, M. J.; Lewis, N. S. *Anal. Chem.*, submitted for publication.

0002-7863/90/1512-1030$02.50/0

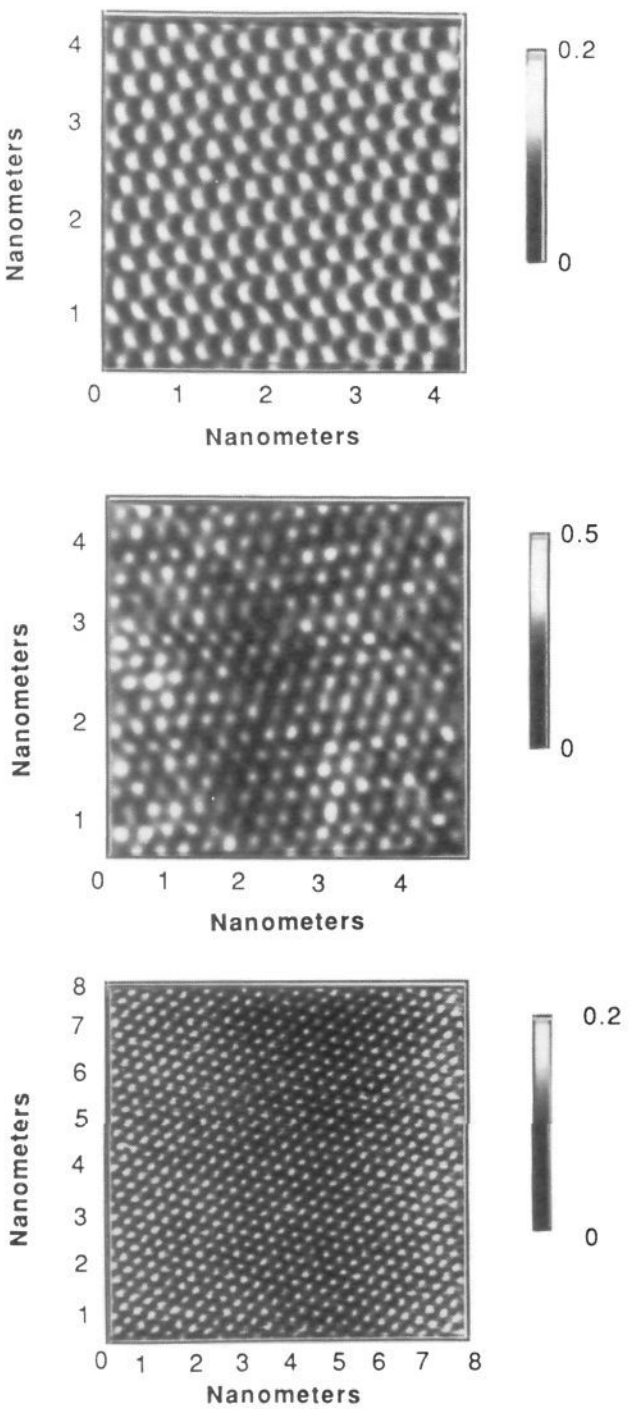

Figure 1. 2D Fourier-filtered STM images of WSe_2 (top), WSeS (middle), and WS_2 (bottom). The images are 44-, 50-, and 82-Å squares, respectively. The voltages were −800, −848, and −510 mV with currents of 2.5, 2.6, and 2.0 nA, respectively. The 2D Fourier filtering was used to remove only high frequencies corresponding to distances below the resolution of the microscope. The *Z* scales shown to the right of each image are shown for comparison only; they do not indicate absolute heights of the atomic features since the images were taken in air.[16]

tip, provided the tip is capable of atomic resolution. The correspondence of the high tunneling current with either the chalcogenide or the metal atoms was the subject of an earlier report and will not be dealt with in detail here.[9] The dilemma may be simply stated as a trade-off between the states energetically accessible to tunneling, associated with the metal d levels comprising the top of the conduction band and the bottom of the valence band, and the much physically closer chalcogenide states (keeping in mind the exponential dependence of tunneling current on distance).

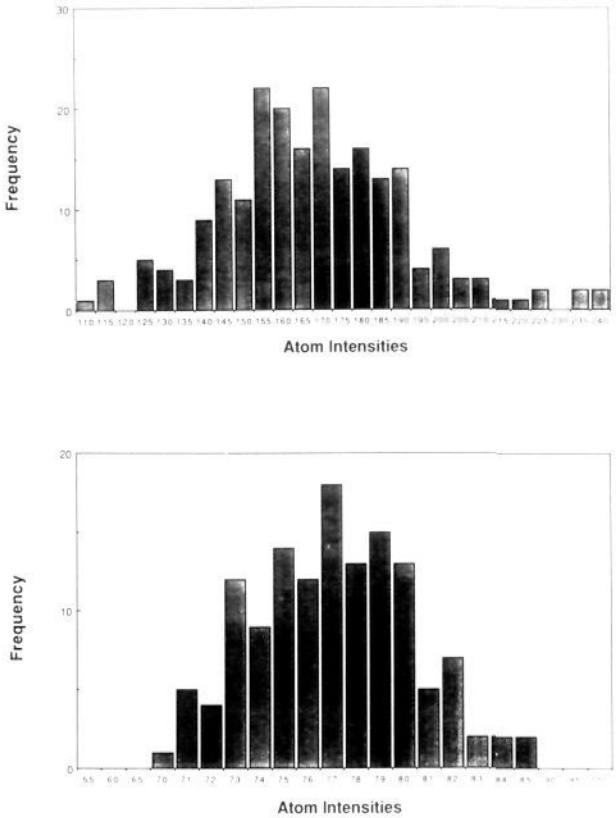

Figure 2. Histograms of atom intensities for WSeS (top) and WSe_2 (bottom). Notice the much wider range of values for the solid solution and that each bar represents a range of five integer values as opposed to the single integer value for the pure solution.

It appears that in metallic compounds (graphite and WTe_2) that the second layer has more influence on the tunneling current, whereas, in the semiconducting materials, the top layer can be imaged. Questions such as these will be the subject of a future report.[13]

The other noticeable aspect of Figure 1 is that the surface atoms are imaged much more uniformly on the homogeneous phases. The pattern of the lighter and darker atoms in the solid-solution images is reproducible from scan to scan except for the normal drift of the entire image. The atom intensity variations suggest that in this case the chalcogenide surface of the layered material is imaged. This will be assumed for the following analysis and discussion although to some extent the model and conclusions would apply to the metal layer also. A statistical analysis of the tunneling currents measured at the atomic peak positions of the 2D Fourier-filtered data resulted in the statistical parameters in Table I for several data sets. The important number is that coefficient of variance for the solid solutions is 3.5–4.2 times larger for the mixed-phase data than for the pure phase. The histograms of atomic tunneling currents for a pure phase and a solid solution are shown in Figure 2.

The wide distribution of atomic intensities in the STM images of the solid solution (Figure 1) does not show a clear distinction between bright atoms and dark atoms, representative of selenium and sulfur atoms. Instead, a distribution of atom intensities is measured, which is not clearly bimodal (Figure 2). Another observation from Figure 1 is that the brightest or darkest atoms are surrounded by other bright or dark atoms. This observation suggests a model where the intensity (tunneling current) at a given atom is related to the nearest-neighbor atoms. A selenium surrounded by other selenium atoms would appear much brighter than a selenium surrounded by sulfurs. The physical reasoning behind such a model is that the electronic interaction between the

(13) Parkinson, B. A. Unpublished results.

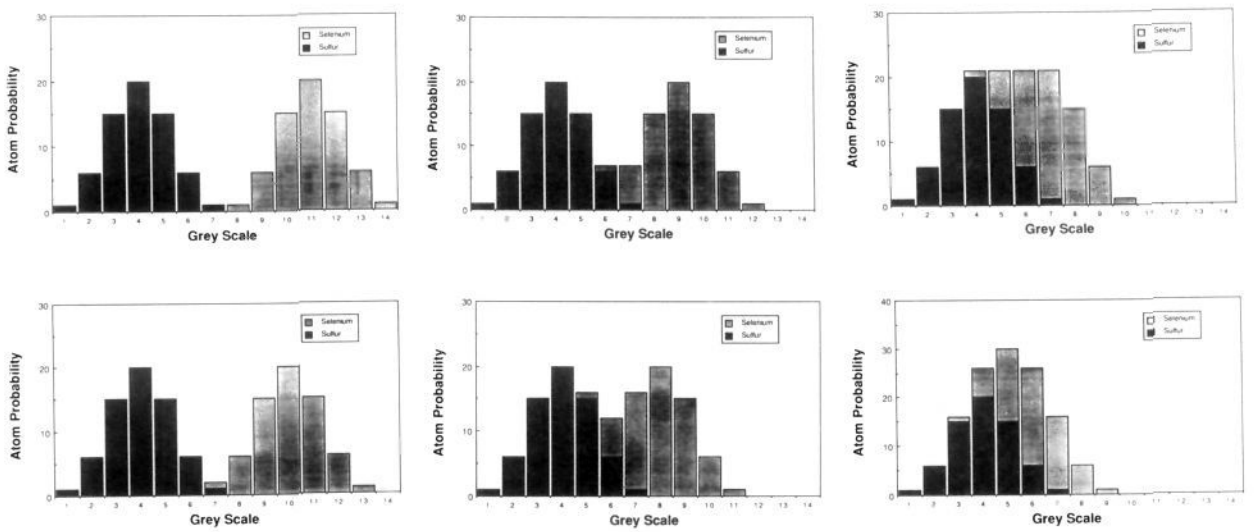

Figure 3. Theoretical histograms of atom intensities based on the binomial distribution of nearest-neighbor atoms and showing various overlaps of the assigned gray scales going from no overlap (upper left) to a 5 gray-scale overlap (lower right).

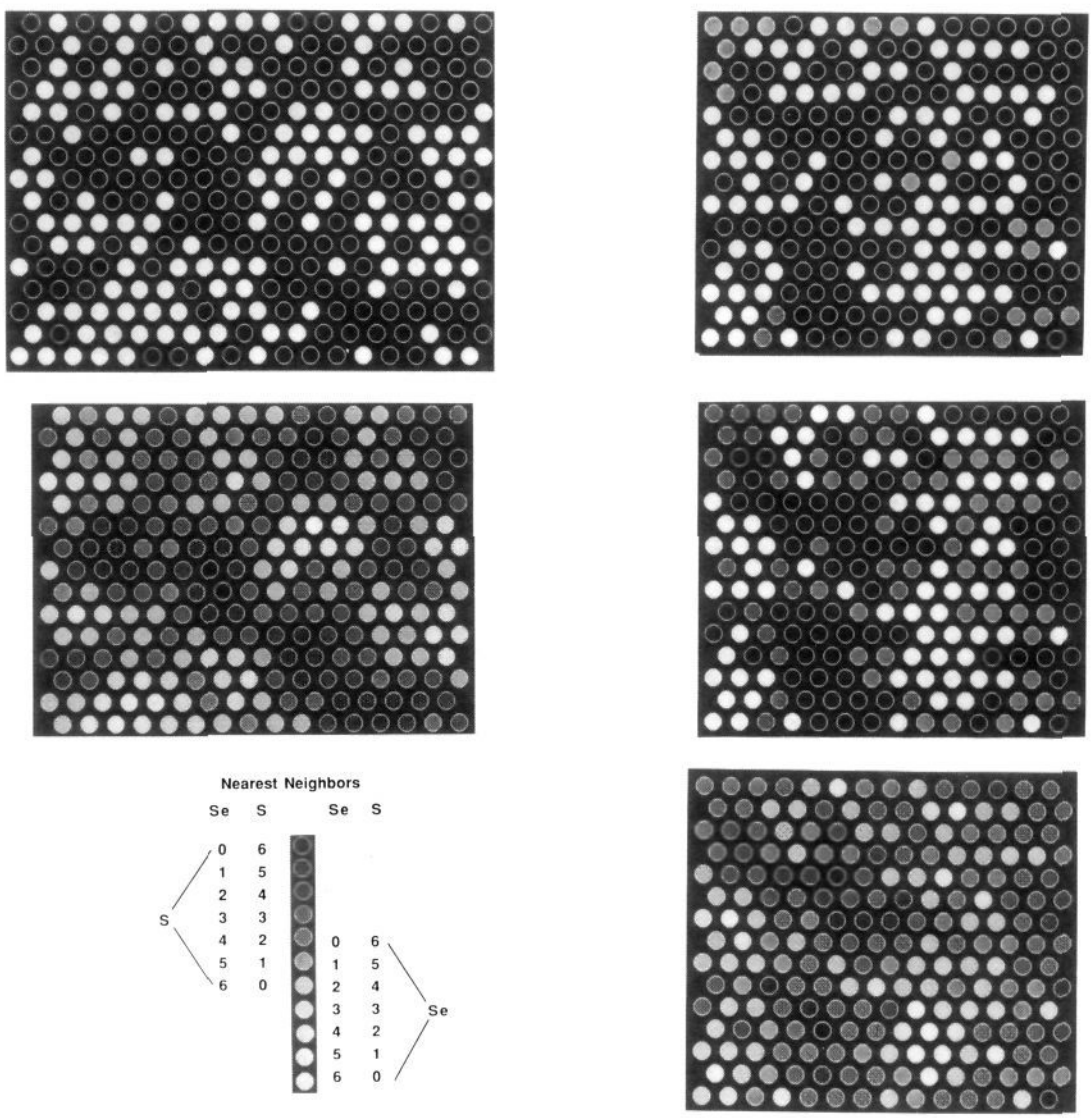

Figure 4. Simulated random selenium (white circles) and sulfur (black circles) occupancies (upper left) and the gray-scale picture from an 11 gray-scale model (middle left; see text) and the gray-scale atom identification key (lower left). Notice that the gray-scale image is smaller since the gray scale of the border atoms cannot be determined. The diagrams on the right are for real STM data transformed to the same 11 gray-scale model as the simulated data (lower right), atom occupancies from the unambiguous gray-scale assignments (middle right), and atom occupancies from application of nearest-neighbor rules (top right).

atoms has a range of about the bond distance but may also be mediated by the shared bonding to subsurface metal atoms.

The finite size of the STM tip is another physical mechanism that could explain the influence of neighboring atoms. A percentage of the tunneling current measured above a sulfur atom could originate from a larger selenium nearest neighbor although a clear image of the sulfur atom is still observed. A simple calculation based only on the exponential dependence of tunneling current on distance and seleniums larger covalent radius (1.02 Å for sulfur and 1.16 Å for selenium) results in a 15% increase in tunneling to the tip from a selenium with the tip at a constant height above the surface. This number should be taken as an upper limit of a purely distance effect since the lattice constants for the *a* and *c* axes are only 3.7 and 5.0% larger, respectively, for the pure selenide phase than for the pure sulfide phase (the lattice constants for the mixed-phase WSeS are 1.85 and 3.3% larger for *a* and *c*).[14] The purely geometric factor cannot account for the large observed differences in tunneling current. This is not surprising since tunneling currents also depend on the density of states as well as on distance. WS_2 has a band gap 0.15 eV larger than WSe_2, suggesting that selenium will have a larger density of states near the Fermi level of the semiconductor.[15] The role of the enhanced modulation effect, observed for STM of graphite imaged in air,[16] on the differential tunneling current between sulfur and selenium is also unknown.

Despite uncertainty about the mechanism of the atomic discrimination, a computer program was written to randomly fill sites with either sulfur or selenium and then simulate images by assigning gray scales proportional to the nearest-neighbor environment for each atom. The probabilities for various nearest-neighbor environments with random filling follow a simple binomial distribution with six like nearest neighbors being least probable and three of each being most probable. Histograms representing such distributions are shown in Figure 3 where the gray scales assigned for each nearest-neighbor environment of sulfur and selenium go from being completely bimodal to having a large overlap. The narrow distribution of atom intensities for the pure phases (Table I) allows us to estimate an error of ±1 gray scale for measurements of the mixed phase. The shape and broadness of the histograms for the mixed phase (i.e., Figure 2) and the theoretical curves (remembering that the distribution is broadened by ±1 gray scale by measurement error) suggest we use a 10 or 11 gray-scale model in the computer simulation. Figure 4 (upper left) shows a simulated occupancy and an 11 gray-scale picture (middle left) with the above described model as well as real data, taken from Figure 1, and plotted in the same fashion as the simulated data (lower right). The simulated and real gray-scale patterns are qualitatively very similar, suggesting the model is appropriate for this system.

Also shown in middle right frame of Figure 4 is the surface site occupancy for the real surface derived from the measured gray scales and assigned by associating the four lightest and four darkest gray scales unambiguously to selenium and sulfur, respectively. About 70% of the atoms can be assign this way (74 sulfur, 71 selenium, and 65 unknown) in agreement with the 11 gray-scale model predicting 34% unassignable atoms (Figure 3). Many of the remaining atoms can be assigned by self-consistent application of nearest-neighbor rules (shown in the upper right frame of Figure 4). For example, an undecided atom surrounded by five or six seleniums is most probably a sulfur since assigning it to a selenium would be an error of 3 or 4 gray scales. The remaining gray atoms represent those that have measurement errors too large to assign them as either selenium or sulfur and most probably have a nearly average nearest-neighbor environment, making them difficult to assign from the nearest-neighbor rules. The model and the derived rules allow for assigning >90% of the surface atoms of several different STM images of WSeS. The majority of the unknown atoms are found at the edges of the frame and cannot be determined from the model because all nearest-neighbor atoms are not seen. If the edge atoms and atoms tied to unknown edge atoms are ignored, >95% of the atoms can be assigned. The assignment including edge atoms (102 sulfurs, 89 seleniums, and 19 unknown atoms) is in remarkable agreement with the determined stoichiometry of the substrate ($WSe_{0.96}S_{1.04}$).

A more sophisticated analysis based on a global examination of the quantitative nearest-neighbor intensities and a complete analysis of the binomial neighbor distribution broadened by the Gaussian measurement errors would allow the assignment of a probability or confidence level for the assignment of each atom. Such an analysis is under development, and we will apply it to a variety of solid-solution compositions where the distribution of nearest neighbors will be highly skewed to one component or the other.

Conclusion

The atomic occupancy and simulated gray-scale images extracted from the data appear to the eye to be very similar to the computer simulations of random occupancy with the use of a very simple nearest-neighbor interaction model. This is not surprising since from X-ray diffraction results WSe_2 and WS_2 are known to form solid solutions throughout the entire composition range[14] so clustering or phase separation would not be expected.

It is interesting to speculate about the composition of the layer immediately above the imaged layer that had been removed via cleavage prior to the experiment. Hints about the 3D ordering of the sulfurs and seleniums across the van der Waals gap could conceivably be obtained if this overlayer could be imaged in the exact spot as the remaining substrate material. The technical difficulty of locating a spot on the cleaveage layer with nanometer accuracy cannot be overestimated. However, if such an experiment could be done, it would be interesting to know whether the nucleation and growth of a new layer during the crystal growth process was templated by the substrate van der Waals surface. There may be a preference for a sulfur to associate with either sulfur or selenium across the van der Waals gap. If such a preference existed, it may be useful as a technique for duplicating information stored at the atomic level by continually regrowing and cleaving new crystals (assuming of course that either the information was somehow encoded in the naturally random atomic pattern or that an artificial means of ordering the surface could be found).

Acknowledgment. Helpful discussions with Jon Caspar are gratefully acknowledged as is the experimental assistance and expert STM tip etching of John Koston. We also thank Nate Lewis for supplying a preprint.

(14) Mentzen, B. F.; Sienko, M. J. *Inorg. Chem.* **1976**, *15*, 2198. Schneemeyer, L. F.; Sienko, M. J. *Inorg. Chem.* **1980**, *19*, 789.
(15) Kam, K.; Parkinson, B. A. *J. Phys. Chem.* **1982**, *82*, 463.
(16) Soler, J. M.; Baro, A. M.; Garcia, N.; Rohrer, H. *Phys. Rev. Lett.* **1986**, *57*, 444. Mamin, H. J.; Ganz, E.; Abraham, D. W.; Thomson, R. E.; Clarke, J. *Phys. Rev. B: Condens. Matter* **1986**, *34*, 9015. Morita, S.; Tsukada, S.; Mikoshiba, N. *Jpn. J. Appl. Phys.* **1987**, *26*, L306.